Scientia Iranica B (2016) 23(6), 2606–2615

Sharif University of Technology
Scientia Iranica
Transactions B: Mechanical Engineering
www.scientiairanica.com

Large-amplitude free vibration of magneto-electro-elastic curved panels

A. Shooshtari* **and S. Razavi**

Department of Mechanical Engineering, Bu-Ali Sina University, Hamedan, P.O. Box 65175-4161, Iran.

Received 13 December 2014; received in revised form 20 October 2015; accepted 28 November 2015

KEYWORDS
Large-amplitude free vibration;
Magneto-electro-elastic material;
Curved panel;
Donnell shell theory;
Multiple timescales method.

Abstract. In this study, the large-amplitude free vibration of magneto-electro-elastic curved panels was investigated. The panel was considered to be simply supported on all edges and the magneto-electro-elastic body was subjected to the electric and magnetic fields along z direction. To obtain the governing equations of motion, the Donnell shell theory and the Gauss's laws for electrostatics and magnetostatics were used. The first mode of vibration of these smart panels was studied in this paper. To this end, the nonlinear partial differential equations of motion were reduced to a nonlinear ordinary differential equation by introducing trial functions for displacements and rotations and then by applying the single-mode Galerkin method on the obtained equation. The resulting equation was solved by multiple timescales perturbation method. Some numerical examples were presented to validate the study and to investigate the effects of several parameters such as geometry of the panel and the magneto-electric boundary conditions on the vibration behavior of these smart panels.

1. Introduction

Magneto-electro-elastic smart materials exhibit a coupling between mechanical, electric, and magnetic fields and are able to convert energy among these energy forms, which makes them suitable for energy harvesting, vibration control, etc.

Static and dynamic responses of piezoelectric plates and shells have been investigated extensively in the past years [1-5]. Pan [6] analyzed the motion of magneto-electro-elastic structures for the first time. Ramirez et al. [7] studied the free vibration of magneto-electro-elastic plates. Razavi and Shooshtari [8] studied the free vibration of a single-layered magneto-electro-elastic shell resting on a Pasternak foundation. Bhangale and Ganesan [9] and Annigeri et al. [10] studied free vibration of simply supported and clamped magneto-electro-elastic cylindrical shells, respectively. Tsai and Wu [11,12] presented free vibration analysis of doubly curved functionally graded magneto-electro-elastic shells with open-circuit and closed-circuit surface conditions, respectively. Chen et al. [13] presented an analytical solution for the static deformation of a magneto-electro-elastic hollow sphere. Xin and Hue [14] presented a semi-analytical model based on the three-dimensional elasticity theory to study the free vibration of simply supported magneto-electro-elastic plates. However, there are few studies dealing with the nonlinear vibration response of magneto-electro-elastic structures. Xue et al. [15] studied the large deflection of a rectangular magneto-electro-elastic thin plate for the first time based on the classical plate theory. Sladek et al. [16] used a meshless local Petrov-Galerkin method to study the large deflection of magneto-electro-elastic thick plates. Milazzo [17] derived a shear deformable model for the large deflection analysis of MEE laminated plates. Alaimo et al. [18] presented an original shear deformable finite-element model for the analysis of large deflections

*. *Corresponding author. Tel.: +98 8138272410*
E-mail address: shooshta@basu.ac.ir (A. Shooshtari)

of magneto-electro-elastic laminated plates. Rao et al. [19] proposed a finite-element model for large deflection static analysis of layered magneto-electro-elastic structures. Razavi and Shooshtari [20] studied nonlinear vibration of symmetrically laminated magneto-electro-elastic rectangular plates. They [21,22] also investigated the effects of electric and magnetic potentials on the nonlinear vibration response of laminated magneto-electro-elastic plates and doubly-curved shells, respectively, with movable simply supported boundary condition. Nonlinear forced vibration of magneto-electro-elastic nanobeams has also been investigated [23,24]. Kattimani and Ray [25,26] studied the active control of large-amplitude vibrations of magneto-electro-elastic plates and doubly curved shell, respectively.

According to the published literature, there are not any studies about the large-amplitude free vibration of multiphase magneto-electro-elastic curved panels. Thus, this study deals with this topic to fill the gap. In this paper the large-amplitude free vibration of a multiphase smart curved panel with immovable simply-supported boundary condition is investigated. The panel is considered to be made of transversely isotropic magneto-electro-elastic material. The magnetic and electric fields are applied along z direction. The Donnell shell theory without in-plane and rotary inertias along with Gauss's laws for electrostatics and magnetostatics is used to model the panel. The first mode of vibration is studied here. To achieve this goal, after transforming the equations of motion to a nonlinear ordinary differential equation by single-mode Galerkin method, it is solved analytically and then a closed-form relation for nonlinear frequency is obtained. This model can be used to study the nonlinear and linear free vibrations of simply-supported single-layered curved panels with magneto-electro-elastic, piezoelectric, piezomagnetic, orthotropic, or isotropic material properties. Several numerical studies are presented to validate the study and to investigate the effects of several parameters on the behavior of these smart panels.

2. Theoretical formulations

For a curved panel with R_x and R_y being the radii of curvature (Figure 1), the strain-displacement relations are given as [27]:

$$\varepsilon_x=\left(u_{0,x}+w_0/R_x+\frac{1}{2}w_{0,x}^2\right)+z\theta_{x,x},$$

$$\varepsilon_y=\left(v_{0,y}+w_0/R_y+\frac{1}{2}w_{0,y}^2\right)+z\theta_{y,y},$$

$$\gamma_{xy}=(u_{0,y}+v_{0,x}+w_{0,x}w_{0,y})+z(\theta_{x,y}+\theta_{y,x}),$$

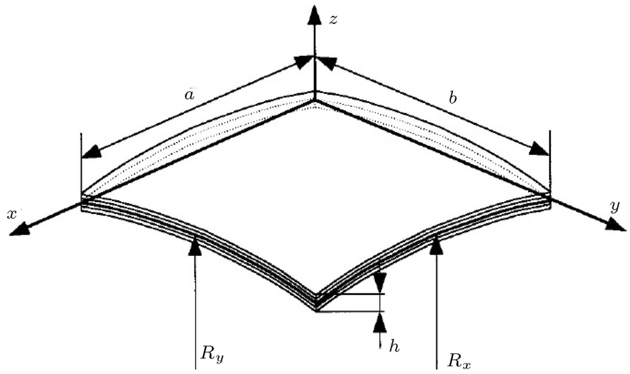

Figure 1. Schematic of the studied curved panel.

$$\gamma_{yz}=w_{0,y}+\theta_y,\qquad \gamma_{xz}=w_{0,x}+\theta_x, \tag{1}$$

where u_0, v_0, and w_0 are the displacements of the mid-surface along x, y, and z directions, respectively, and θ_x and θ_y are the rotations of a transverse normal about the y and x directions, respectively.

Assuming that the electric and magnetic fields are applied along z-direction, the constitutive equations of transversely isotropic magneto-electro-elastic panel can be written in the following form [6]:

$$\begin{Bmatrix}\sigma_x\\ \sigma_y\\ \sigma_{xz}\\ \sigma_{yz}\\ \sigma_{xy}\end{Bmatrix}=\begin{bmatrix}C_{11}&C_{12}&0&0&0\\ C_{12}&C_{22}&0&0&0\\ 0&0&C_{55}&0&0\\ 0&0&0&C_{44}&0\\ 0&0&0&0&C_{66}\end{bmatrix}\begin{Bmatrix}\varepsilon_x\\ \varepsilon_y\\ \gamma_{xz}\\ \gamma_{yz}\\ \gamma_{xy}\end{Bmatrix}+\begin{bmatrix}0&0&e_{31}\\ 0&0&e_{32}\\ 0&e_{24}&0\\ e_{15}&0&0\\ 0&0&0\end{bmatrix}\begin{Bmatrix}0\\ 0\\ \phi_{,z}\end{Bmatrix}+\begin{bmatrix}0&0&q_{31}\\ 0&0&q_{32}\\ 0&q_{24}&0\\ q_{15}&0&0\\ 0&0&0\end{bmatrix}\begin{Bmatrix}0\\ 0\\ \psi_{,z}\end{Bmatrix}, \tag{2}$$

$$\begin{Bmatrix}D_x\\ D_y\\ D_z\end{Bmatrix}=\begin{bmatrix}0&0&0&e_{15}&0\\ 0&0&e_{24}&0&0\\ e_{31}&e_{32}&0&0&0\end{bmatrix}\begin{Bmatrix}\varepsilon_x\\ \varepsilon_y\\ \gamma_{xz}\\ \gamma_{yz}\\ \gamma_{xy}\end{Bmatrix}-\begin{bmatrix}\eta_{11}&0&0\\ 0&\eta_{22}&0\\ 0&0&\eta_{33}\end{bmatrix}\begin{Bmatrix}0\\ 0\\ \phi_{,z}\end{Bmatrix}-\begin{bmatrix}d_{11}&0&0\\ 0&d_{22}&0\\ 0&0&d_{33}\end{bmatrix}\begin{Bmatrix}0\\ 0\\ \psi_{,z}\end{Bmatrix}, \tag{3}$$

$$\begin{Bmatrix} B_x \\ B_y \\ B_z \end{Bmatrix} = \begin{bmatrix} 0 & 0 & 0 & q_{15} & 0 \\ 0 & 0 & q_{24} & 0 & 0 \\ q_{31} & q_{32} & 0 & 0 & 0 \end{bmatrix} \begin{Bmatrix} \varepsilon_x \\ \varepsilon_y \\ \gamma_{xz} \\ \gamma_{yz} \\ \gamma_{xy} \end{Bmatrix} - \begin{bmatrix} d_{11} & 0 & 0 \\ 0 & d_{22} & 0 \\ 0 & 0 & d_{33} \end{bmatrix} \begin{Bmatrix} 0 \\ 0 \\ \phi_{,z} \end{Bmatrix} - \begin{bmatrix} \mu_{11} & 0 & 0 \\ 0 & \mu_{22} & 0 \\ 0 & 0 & \mu_{33} \end{bmatrix} \begin{Bmatrix} 0 \\ 0 \\ \psi_{,z} \end{Bmatrix}, \tag{4}$$

where $\{\sigma_x \quad \sigma_y \quad \sigma_{xz} \quad \sigma_{yz} \quad \sigma_{xy}\}^T$ is stress vector; $\{D_x \quad D_y \quad D_z\}^T$ and $\{B_x \quad B_y \quad B_z\}^T$ are the electric displacement and magnetic flux density vectors, respectively; $[C_{ij}]$, $[\eta_{ij}]$, and $[\mu_{ij}]$ are the elastic, dielectric, and magnetic permeability coefficient matrices, respectively; $[e_{ij}]$, $[q_{ij}]$, and $[d_{ij}]$ are the piezoelectric, piezomagnetic, and magneto-electric coefficient matrices, respectively; and ϕ and ψ are electric and magnetic potentials.

By neglecting in-plane and rotary inertia effects, the equations of motion of a curved panel can be expressed in the following form [27]:

$$N_{x,x} + N_{xy,y} = 0, \tag{5}$$

$$N_{xy,x} + N_{y,y} = 0, \tag{6}$$

$$Q_{x,x} + Q_{y,y} + (N_x w_{0,x} + N_{xy} w_{0,y})_{,x} + (N_{xy} w_{0,x} + N_y w_{0,y})_{,y} - N_x/R_x - N_y/R_y = I_0 w_{0,tt}, \tag{7}$$

$$M_{x,x} + M_{xy,y} - Q_x = 0, \tag{8}$$

$$M_{xy,x} + M_{y,y} - Q_y = 0, \tag{9}$$

where $I_0 = \int_{-h/2}^{h/2} \rho_0 dz$ is the mass moment of inertia, in which ρ_0 is the density of the material of the panel. The in-plane force resultants (i.e., N_x, N_y, N_{xy}), the transverse force resultants (i.e., Q_x, Q_y) and the moment resultants (i.e., M_x, M_y, M_{xy}) are obtained by the following equations:

$$\{N_x \quad N_y \quad N_{xy}\}^T = \int_{-h/2}^{h/2} \{\sigma_x \quad \sigma_y \quad \sigma_{xy}\}^T dz,$$

$$\{M_x \quad M_y \quad M_{xy}\}^T = \int_{-h/2}^{h/2} \{\sigma_x \quad \sigma_y \quad \sigma_{xy}\}^T z dz,$$

$$\{Q_x \quad Q_y\}^T = K \int_{-h/2}^{h/2} \{\sigma_{xz} \quad \sigma_{yz}\}^T dz, \tag{10}$$

where K is shear correction factor.

To obtain the resultants of Eq. (10), the gradients of the electric and magnetic potentials in Eq. (2) must be obtained in terms of z. To this end, Gauss's laws for electrostatics and magnetostatics, i.e.:

$$D_{x,x} + D_{y,y} + D_{z,z} = 0, \tag{11}$$

$$B_{x,x} + B_{y,y} + B_{z,z} = 0, \tag{12}$$

along with Eqs. (3) and (4) are considered from which one obtains:

$$\phi = M_1 z^2 + \phi_0 z + \phi_1, \qquad \psi = M_2 z^2 + \psi_0 z + \psi_1. \tag{13}$$

In the above equation, M_1 and M_2 are obtained by:

$$M_1 = \frac{1}{2}\left(a_1 w_{0,xx} + a_2 w_{0,yy} + a_3 \theta_{x,x} + a_4 \theta_{y,y}\right), \tag{14}$$

$$M_2 = \frac{1}{2}\left(a_5 w_{0,xx} + a_6 w_{0,yy} + a_7 \theta_{x,x} + a_8 \theta_{y,y}\right), \tag{15}$$

where:

$$\delta_1 = d_{33}/(d_{33}^2 - \mu_{33}\eta_{33}),$$

$$\delta_2 = \mu_{33}/(d_{33}^2 - \mu_{33}\eta_{33}),$$

$$\delta_3 = \eta_{33}/(d_{33}^2 - \mu_{33}\eta_{33}),$$

$$a_1 = \delta_1 q_{15} - \delta_2 e_{15},$$

$$a_2 = \delta_1 q_{24} - \delta_2 e_{24},$$

$$a_3 = \delta_1 (q_{15} + q_{31}) - \delta_2 (e_{15} + e_{31}),$$

$$a_4 = \delta_1 (q_{24} + q_{31}) - \delta_2 (e_{24} + e_{31}),$$

$$a_5 = \delta_1 e_{15} - \delta_3 q_{15}, \qquad a_6 = \delta_1 e_{24} - \delta_3 q_{24},$$

$$a_7 = \delta_1 (e_{15} + e_{31}) - \delta_3 (q_{15} + q_{31}),$$

$$a_8 = \delta_1 (e_{24} + e_{31}) - \delta_3 (q_{24} + q_{31}). \tag{16}$$

On the other hand, the integration constants, i.e. ϕ_0, ϕ_1, ψ_0, and ψ_1, are obtained by applying the magneto-electric boundary condition on top and bottom surfaces of the plate.

Closed-circuit and open-circuit magneto-electric boundary conditions are considered in this study. These boundary conditions are expressed in the following form:

$$\phi = \psi = 0, \qquad (z = \pm h/2) \quad \text{(closed-circuit)}, \tag{17}$$

$$B_z = D_z = 0, \qquad (z = \pm h/2) \quad \text{(open-circuit)}. \tag{18}$$

Eqs. (5)-(10) and (13) give the Partial Differential Equations (PDEs) of motion in terms of displacements

Table 1. Dimensionless fundamental frequencies of curved isotropic panels ($a = b$, $a = 10h$, and $\nu = 0.3$).

R_x/a	R_y/b	Alijani et al. [29]	Chorfi and Houmat [30]	Matsunaga [31]	Bich et al. [32]	Bich et al. [33]	Present study
∞	∞	0.0597	0.0577	0.0588	0.0597	0.0581	0.05812
2	∞	0.0648	0.0629	0.0622	0.0648	0.0632	0.06327
2	2	0.0779	0.0762	0.0751	—	0.0767	0.07667
-2	2	0.0597	0.0580	0.0563	—	0.0592	0.05812

and rotations. The immovable simply supported boundary condition is expressed in the following form:

$$u_0 = v_0 = w_0 = \theta_y = w_{0,xx} = 0 \quad \text{at} \quad x = 0, a,$$

$$u_0 = v_0 = w_0 = \theta_x = w_{0,yy} = 0 \quad \text{at} \quad y = 0, a, \tag{19}$$

for which the displacements and rotations can be obtained by:

$$\begin{Bmatrix} u_0 \\ v_0 \\ w_0 \\ \theta_x \\ \theta_y \end{Bmatrix} = \begin{Bmatrix} hU\sin(2\pi x/a)\sin(\pi y/b) \\ hV\sin(\pi x/a)\sin(2\pi y/b) \\ hW\sin(\pi x/a)\sin(\pi y/b) \\ X\cos(\pi x/a)\sin(\pi y/b) \\ Y\sin(\pi x/a)\cos(\pi y/b) \end{Bmatrix}, \tag{20}$$

and by applying the Galerkin method to the PDEs of motion, one obtains:

$$L_1W^2 + L_2W + L_3U + L_4V = 0, \tag{21}$$

$$L_5W^2 + L_6W + L_7U + L_8V = 0, \tag{22}$$

$$L_9W^3 + L_{10}W^2 + L_{11}UW + L_{12}VW + L_{13}V + L_{14}U + L_{15}X + L_{16}Y + L_{17}W + L_{18}\ddot{W} = 0, \tag{23}$$

$$L_{19}W + L_{20}X + L_{21}Y = 0, \tag{24}$$

$$L_{22}W + L_{23}X + L_{24}Y = 0, \tag{25}$$

where L_i ($i = 1, 2, \cdots, 24$) are constant coefficients and are given in Appendix A for two magneto-electric boundary conditions.

Obtaining U and V from Eqs. (21) and (22), and X and Y from Eqs. (24) and (25), and then substituting the obtained values into Eq. (23) give:

$$\ddot{W} + \omega_0^2 W + \alpha W^2 + \beta W^3 = 0, \tag{26}$$

where the coefficients are given in Appendix B.

Eq. (26) can be analytically solved by using multiple timescales method. To do this, a small dimensionless parameter (ε) is inserted to Eq. (26) to scale the nonlinear terms [28]:

$$\ddot{W} + \omega_0^2 W = -\varepsilon \alpha W^2 - \varepsilon^2 \beta W^3. \tag{27}$$

Solving Eq. (27), one can simply obtain the nonlinear frequency ratio [28]:

$$\omega_{\mathrm{NL}}/\omega_{\mathrm{L}} = \left[1 + \frac{9\beta\omega_0^2 - 10\alpha}{12\omega_0^4} p_0^2\right]^{1/2}, \tag{28}$$

where $p_0 = w_{\max}/h$ is the dimensionless initial displacement.

3. Results and discussion

In the numerical examples, the shear correction factor (K) is taken to be 5/6. Dimensionless fundamental frequencies, $\omega = \omega_0 h\sqrt{\rho_0/E}$, of curved isotropic panels for different radii of curvature are obtained and compared with the previously published results (Table 1). The results of the presented model are compared with the results of Alijani et al. [29] based on the Donnell's nonlinear shallow shell theory, Chorfi and Houmat [30] based on the first-order shear deformation theory, Matsunaga [31] based on the two-dimensional higher-order theory, and Bich et al. [32,33] based on the classical shell theory and first-order shear deformation theory, respectively. It is seen that although the panels are relatively thick, the results are in good agreement with the higher-order results reported by Matsunaga [31].

Table 2 shows the dimensionless frequencies of piezoelectric $BaTiO_3$ and piezomagnetic $CoFe_2O_4$ square thick plates, which are compared with the results obtained by higher-order shear deformation theory [34] and 3D approach [35]. For $BaTiO_3$, the material properties are: $C_{11} = C_{22} = 166$ GPa, $C_{12} = 77$ GPa, $C_{44} = C_{55} = 43$ GPa, $C_{66} = 44.5$ GPa, $e_{31} = e_{32} = -4.4$ Cm^{-2}, $e_{15} = e_{24} = 11.6$ Cm^{-2}, $\eta_{33} = 12.6 \times 10^{-9}$ C(Vm)$^{-1}$, $\mu_{33} = 10 \times 10^{-6}$ Ns^{2}C^{-2}, and $\rho_0 = 5800$ kgm^{-3}; and the material properties of $CoFe_2O_4$ are: $C_{11} = C_{22} = 286$ GPa, $C_{12} = 173$ GPa, $C_{44} = C_{55} = 45.3$ GPa, $C_{66} =$

Table 2. Dimensionless fundamental frequencies of piezoelectric and piezomagnetic thick plates ($R_x = R_y = \infty$).

Method	$BaTiO_3$	$CoFe_2O_4$
HSDT [34]	1.2629	1.1358
3D [35]	1.2660	1.0212
Present study	1.3268	1.1735

56.5 GPa, $q_{31} = q_{32} = 580.3$ N(Am)$^{-1}$, $q_{15} = q_{24} =$ 550 N(Am)$^{-1}$, $\eta_{33} = 0.093 \times 10^{-9}$ C(Vm)$^{-1}$, $\mu_{33} =$ 157 $\times$ 10^{-6} Ns^{2}C^{-2}, and $\rho_0 = 5300$ kgm^{-3}. The geometric properties of the plates are $a = b = 1$ m and $h = 0.3$ m, and the dimensionless frequencies are obtained by $\omega = \omega_0 a\sqrt{\rho_0/C_{\max}}$, where $C_{\max}$ denotes the maximum of C_{ij} of the material of the plate. There is a discrepancy between the results of the present study with highly accurate HSDT and 3D results. This is because the plates are thick and the rotary inertia is not included in the formulation. Thus, the proposed approach can predict the vibration of thin and relatively thick panels with an acceptable precision.

As the last comparison, the nonlinear frequency ratios ($\omega_{\mathrm{NL}}/\omega_{\mathrm{L}}$) of an isotropic square plate with immovable simply-supported boundary condition are obtained and compared with the results obtained by a shear deformable finite-element model [36] (Table 3). Good agreement is observed between the results of the present approach and the ones obtained by Singha and Daripa [36].

In Tables 4 and 5, the nonlinear frequency ratios of magneto-electro-elastic curved panels with the following material properties are presented [37]: $C_{11} =$ 226 GPa, $C_{12} = 124$ GPa, $C_{22} = 216$ GPa, $C_{44} =$ $C_{55} = 44$ GPa, $C_{66} = 51$ GPa, $e_{31} = e_{32} =$ -2.2 Cm^{-2}, $q_{31} = q_{32} = 290.2$ N(Am)$^{-1}$, $\eta_{33} = 6.35 \times 10^{-9}$ C(Vm)$^{-1}$, $d_{33} = 2737.5 \times 10^{-12}$ Ns(CV)$^{-1}$, $\mu_{33} =$ 83.5 $\times$ 10^{-6} Ns^{2}C^{-2}, and $\rho_0 = 5500$ kgm^{-3}. Three curved panels are considered in these tables, which are spherical, cylindrical, and hyperbolic paraboloidal panels. The hyperbolic paraboloidal panel has the highest and spherical panel has the lowest nonlinear frequency ratios among the three panels. Moreover, it is seen that the nonlinear frequency ratio is slightly higher for the open-circuit magneto-electric boundary condition, which means that in the open-circuit boundary condition, the nonlinearity of the panel is more than that of the closed-circuit case. However, the spherical panel has the same nonlinear behavior in the open-circuit and closed-circuit cases for vibration amplitudes equal to or smaller than the shell thickness. By contrast, magneto-electric boundary condition has the greatest effect on the response of hyperbolic paraboloidal panel.

The effect of panel thickness on the response has also been investigated and the results are shown in Tables 6 and 7. For each panel a/b, a/h, R_x/a, and R_y/b, ratios are constant whereas h can be changed. It is seen that thinner spherical and cylindrical panels have higher nonlinear frequency ratios. However, no change is observed in the nonlinear frequency ratio of the hyperbolic paraboloidal panel.

In Figure 2, backbone curves of piezoelectric $BaTiO_3$, piezomagnetic $CoFe_2O_4$, and magneto-electro-elastic panels are presented. The magneto-electric boundary condition is considered to be closed-circuit. It is observed that for the spherical panel, the backbone curves of magneto-electro-elastic and

Table 3. Nonlinear frequency ratios of an isotropic square plate ($a/h = 100$, $\nu = 0.3$, and $R_x = R_y = \infty$).

Method	$w_{\max}/h$				
	0.2	**0.4**	**0.6**	**0.8**	**1.0**
Singha and Daripa [36]	1.01967	1.07669	1.16597	1.28131	1.41684
Present study	1.02085	1.08099	1.17440	1.29389	1.43295

Table 4. Nonlinear frequency ratios of curved panels with open-circuit magneto-electric boundary condition ($a = b = 100h$).

R_x/a	R_y/b	$w_{\max}/h$				
		0.2	**0.4**	**0.6**	**0.8**	**1.0**
2	2	1.00013	1.00050	1.00113	1.00201	1.00313
2	∞	1.00036	1.00145	1.00326	1.00579	1.00904
-2	2	1.00038	1.00151	1.00339	1.00602	1.00939

Table 5. Nonlinear frequency ratios of curved panels with closed-circuit magneto-electric boundary condition ($a = b = 100h$).

R_x/a	R_y/b	$w_{\max}/h$				
		0.2	**0.4**	**0.6**	**0.8**	**1.0**
2	2	1.00013	1.00050	1.00113	1.00201	1.00313
2	∞	1.00036	1.00145	1.00325	1.00578	1.00902
-2	2	1.00037	1.00150	1.00336	1.00597	1.00931

Table 6. Nonlinear frequency ratios of open-circuit magneto-electric curved panels with different thicknesses ($a = b = 100h$).

R_x/a	R_y/b	$w_{\max}/h$			
		0.6		**1.0**	
		h		h	
		0.1	**1.0**	**0.1**	**1.0**
2	2	1.00114	1.00113	1.00317	1.00313
2	∞	1.00331	1.00326	1.00917	1.00904
-2	2	1.00339	1.00339	1.00939	1.00939

Table 7. Nonlinear frequency ratios of closed-circuit magneto-electric curved panels with different thicknesses ($a = b = 100h$).

R_x/a	R_y/b	$w_{\max}/h$			
		0.6		**1.0**	
		h		h	
		0.1	**1.0**	**0.1**	**1.0**
2	2	1.00114	1.00113	1.00317	1.00313
2	∞	1.00330	1.00325	1.00915	1.00902
-2	2	1.00336	1.00336	1.00931	1.00931

$CoFe_2O_4$ panels are almost identical. Moreover, in cylindrical and hyperbolic paraboloidal panels, $CoFe_2O_4$ and $BaTiO_3$ have the most and the least nonlinearity, respectively.

4. Conclusions

Large-amplitude free vibration of magneto-electro-elastic curved panels is investigated in this paper. The Donnell shell theory, Gauss's laws for electrostatics and magnetostatics, and Galerkin and multiple timescales methods are used to model and solve the problem. The effects of geometry of the panel and the magneto-electric boundary conditions on the vibration behavior of these smart panels are studied by using some numerical examples and it is found that:

(a) The hyperbolic paraboloidal panel has the most and spherical panel has the least nonlinear frequency ratio among the spherical, cylindrical, and hyperbolic paraboloidal panels;

(b) The nonlinear frequency ratio is higher for the open-circuit magneto-electric boundary condition, meaning that in the open-circuit case, the nonlinearity of the panel is more than that of the closed-circuit case;

(c) Thinner spherical and cylindrical panels have higher nonlinear frequency ratios;

(d) Backbone curves of magneto-electro-elastic and $CoFe_2O_4$ spherical panels are almost identical.

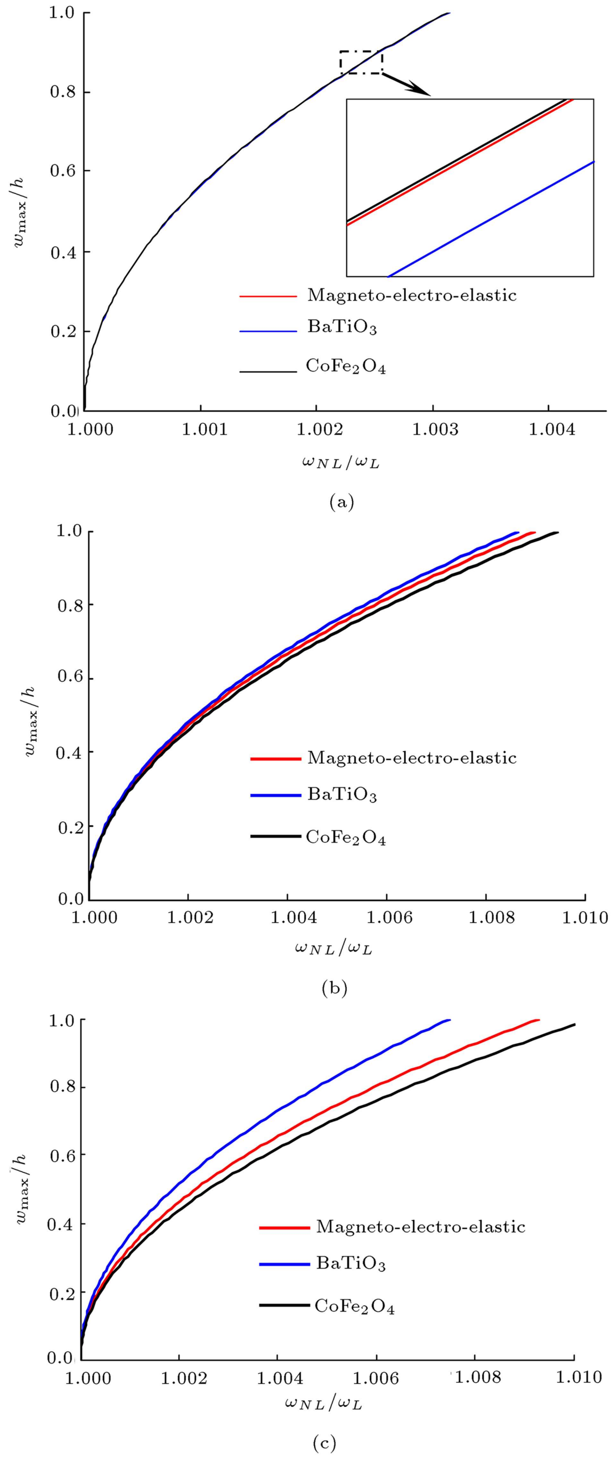

Figure 2. Backbone curves of (a) spherical, (b) cylindrical, and (c) hyperbolic paraboloidal panels with closed-circuit magneto-electric boundary conditions ($a = b = 100h$).

References

1. Alibeigloo, A. and Kani, A.M. "3D free vibration analysis of laminated cylindrical shell integrated piezoelectric layers using the differential quadrature method", *Appl. Math. Model.*, **34**(12), pp. 4123-4137 (2010).

2. Behjat, B., Salehi, M., Armina, A., Sadighi, M. and Abbasi, M. "Static and dynamic analysis of functionally graded piezoelectric plates under mechanical and electrical loading", *Sci. Iran.*, **18**(4), pp. 986-994 (2011).

3. Jafari, A.A., Khalili, S.M.R. and Tavakolian, M. "Nonlinear vibration of functionally graded cylindrical shells embedded with a piezoelectric layer", *Thin Wall. Struct.*, **79**, pp. 8-15 (2014).

4. Akbari Alashti, R., Khorsand, M. and Tarahhomi, M.H. "Thermo-elastic analysis of a functionally graded spherical shell with piezoelectric layers by differential quadrature method", *Sci. Iran.*, **20**(1), pp. 109-119 (2013).

5. Shen, H.S. and Yang, D.Q. "Nonlinear vibration of anisotropic laminated cylindrical shells with piezoelectric fiber reinforced composite actuators", *Ocean Eng.*, **80**, pp. 36-49 (2014).

6. Pan, E. "Exact solution for simply supported and multilayered magneto-electro-elastic plates", *J. Appl. Mech.*, **68**(4), pp. 608-618 (2001).

7. Ramirez, F., Heyliger, P.R. and Pan, E. "Discrete layer solution to free vibrations of functionally graded magneto-electro-elastic plates", *Mech. Adv. Mater. Struc.*, **13**(3), pp. 249-266 (2006).

8. Razavi, S. and Shooshtari, A. "Free vibration analysis of a magneto-electro-elastic doubly-curved shell resting on a Pasternak-type elastic foundation", *Smart Mater. Struct.*, **23**(10), 105003 (2014).

9. Bhangale, R.K. and Ganesan, N. "Free vibration studies of simply supported non-homogeneous functionally graded magneto-electro-elastic finite cylindrical shells", *J. Sound Vib.*, **288**(1-2), pp. 412-422.

10. Annigeri, A.R., Ganesan, N. and Swarnamani, S. "Free vibrations of clamped-clamped magneto-electro-elastic cylindrical shells", *J. Sound Vib.*, **292**(1-2), pp. 300-314 (2006).

11. Tsai, Y.H. and Wu, C.P. "Dynamic responses of functionally graded magneto-electro-elastic shells with open-circuit surface conditions", *Int. J. Eng. Sci.*, **46**(9), pp. 843-857 (2008).

12. Wu, C.P. and Tsai, Y.H. "Dynamic responses of functionally graded magneto-electro-elastic shells with closed-circuit surface conditions using the method of multiple scales", *Eur. J. Mech. A-Solid.*, **29**(2), pp. 166-181 (2010).

13. Chen, J.Y., Pan, E. and Heyliger, P.R. "Static deformation of a spherically anisotropic and multilayered magneto-electro-elastic hollow sphere", *Int. J. Solids Struct.*, **60-61**, pp. 66-74 (2015).

14. Xin, L. and Hu, Z. "Free vibration of simply supported and multilayered magneto-electro- elastic plates", *Compos. Struct.*, **121**, pp. 344-350 (2015).

15. Xue, C.X., Pan, E., Zhang, S.Y. and Chu, H.J. "Large deflection of a rectangular magnetoelectroelastic thin plate", *Mech. Res. Commun.*, **38**(7), pp. 518-523 (2011).

16. Sladek, J., Sladek, V., Krahulec, S. and Pan, E. "The MLPG analyses of large deflections of magnetoelectroelastic plates", *Eng. Anal. Bound. Elem.*, **37**(4), pp. 673-682 (2013).

17. Milazzo, A. "Large deflection of magneto-electro-elastic laminated plates", *Appl. Math. Model.*, **38**(5-6), pp. 1737-1752 (2014).

18. Alaimo, A., Benedetti, I. and Milazzo, A. "A finite element formulation for large deflection of multilayered magneto-electro-elastic plates", *Compos. Struct.*, **107**, pp. 643-653 (2014).

19. Rao, M.N., Schmidt, R. and Schröder, K.U. "Geometrically nonlinear static FE-simulation of multilayered magneto-electro-elastic composite structures", *Compos. Struct.*, **127**, pp. 120-131 (2015).

20. Razavi, S. and Shooshtari, A. "Nonlinear free vibration of magneto-electro-elastic rectangular plates", *Compos. Struct.*, **119**, pp. 377-384 (2015).

21. Shooshtari, A. and Razavi, S. "Large amplitude free vibration of symmetrically laminated magneto-electro-elastic rectangular plates on Pasternak type foundation", *Mech. Res. Commun.*, **69**, pp. 103-113 (2015).

22. Shooshtari, A. and Razavi, S. "Linear and nonlinear free vibration of a multilayeredmagneto-electro-elastic doubly-curved shell on elastic foundation", *Compos. Part B-Eng.*, **78**, pp. 95-108 (2015).

23. Ansari, R., Hasrati, E., Gholami, R. and Sadeghi, F. "Nonlinear analysis of forced vibration of nonlocal third-order shear deformable beam model of magneto-electro-thermo elastic nanobeams", *Compos. Part B-Eng.*, **83**, pp. 226-241 (2015).

24. Ansari, R., Gholami, R. and Rouhi, H. "Size-dependent nonlinear forced vibration analysis of magneto-electro-thermo-elastic Timoshenko nanobeams based upon the nonlocal elasticity theory", *Compos. Struct.*, **126**, pp. 216-226 (2015).

25. Kattimani, S.C. and Ray, M.C. "Control of geometrically nonlinear vibrations of functionally graded magneto-electro-elastic plates", *Int. J. Mech. Sci.*, **99**, pp. 154-167 (2015).

26. Kattimani, S.C. and Ray, M.C. "Active control of large amplitude vibrations of smart magneto-electro-elastic doubly curved shells", *Int. J. Mech. Mater. Des.*, **10**(4), pp. 351-378 (2014).

27. Reddy, J.N., *Mechanics of Laminated Composite Plates and Shells: Theory and Analysis*, 2nd Ed. pp. 621-622, CRC Press (2004).

28. Nayfeh, A.H. and Mook, D.T., *Nonlinear Oscillations*, pp. 195-198, John Wiley & Sons, Inc. (1995).

29. Alijani, F., Amabili, M., Karagiozis, K. and Bakhtiari-Nejad, F. "Nonlinear vibrations of functionally graded-doubly curved shallow shells", *J. Sound Vib.*, **330**(7), pp. 1432-1454 (2011).

30. Chorfi, S.M. and Houmat, A. "Nonlinear free vibration of a functionally graded doubly curved shallow shell of elliptical plan-form", *Compos. Struct.*, **92**(10), pp. 2573-2581 (2010).
31. Matsunaga, H. "Free vibration and stability of functionally graded shallow shells according to a 2-D higher-order deformation theory", *Compos. Struct.*, **84**(2), pp. 132-146 (2008).
32. Bich, D.H., Dung, D.V. and Nam, V.H. "Nonlinear dynamical analysis of eccentrically stiffened functionally graded cylindrical panels", *Compos. Struct.*, **94**(8), pp. 2465-2473 (2012).
33. Bich, D.H., Duc, N.D. and Quan, T.Q. "Nonlinear vibration of imperfect eccentrically stiffened functionally graded double curved shallow shells resting on elastic foundation using the first order shear deformation theory", *Int. J. Mech. Sci.*, **80**, pp. 16-28 (2014).
34. Moita, J.M.S., Soares, C.M.M. and Soares, C.A.M. "Analyses of magneto-electro-elastic plates using a higher order finite element model", *Compos. Struct.*, **91**(4), pp. 421-426 (2009).
35. Wu, C.P. and Lu, Y.C. "A modified Pagano method for the 3D dynamic responses of functionally graded magneto-electro-elastic plates", *Compos. Struct.*, **90**(3), pp. 363-372 (2009).
36. Singha, M.K. and Daripa, R. "Nonlinear vibration and dynamic stability analysis of composite plates", *J. Sound. Vib.*, **328**(4-5), pp. 541-554 (2009).
37. Li, Y. and Zhang, J. "Free vibration analysis of magnetoelectroelastic plate resting on a Pasternak foundation", *Smart Mater. Struct.*, **23**(2), 025002 (2014).

Appendix A

$$\lambda_1 = (d_{33}q_{31} - \mu_{33}e_{31})/(d_{33}^2 - \mu_{33}\eta_{33}),$$
$$\lambda_2 = (d_{33}e_{31} - \eta_{33}q_{31})/(d_{33}^2 - \mu_{33}\eta_{33}). \tag{A.1}$$

For the open-circuit boundary condition we have the following equations:

$$\begin{aligned}
L_1 =& \frac{\pi^2 h^3}{6b}(C_{12} - C_{66} + e_{31}\lambda_1 + q_{31}\lambda_2) \\
&- \frac{\pi^2 bh^3}{3a^2}(C_{11} + e_{31}\lambda_1 + q_{31}\lambda_2), \\
L_2 =& \frac{2bh^2}{3R_x}(C_{11} + e_{31}\lambda_1 + q_{31}\lambda_2) \\
&+ \frac{2bh^2}{3R_y}(C_{12} + e_{31}\lambda_1 + q_{31}\lambda_2), \\
L_3 =& -\frac{\pi^2 bh^2}{a}(C_{11} + e_{31}\lambda_1 + q_{31}\lambda_2) - \frac{\pi^2 ah^2}{4b}C_{66}, \\
L_4 =& -\frac{16h^2}{9}(C_{12} + C_{66} + e_{31}\lambda_1 + q_{31}\lambda_2),
\end{aligned} \tag{A.2}$$

$$\begin{aligned}
L_5 =& \frac{\pi^2 h^3}{6a}(C_{12} - C_{66} + e_{32}\lambda_1 + q_{32}\lambda_2) \\
&- \frac{\pi^2 ah^3}{3b^2}(C_{22} + e_{32}\lambda_1 + q_{32}\lambda_2), \\
L_6 =& \frac{2ah^2}{3R_x}(C_{12} + e_{32}\lambda_1 + q_{32}\lambda_2) \\
&+ \frac{2ah^2}{3R_y}(C_{22} + e_{32}\lambda_1 + q_{32}\lambda_2), \\
L_7 =& -\frac{16h^2}{9}(C_{12} + C_{66} + e_{32}\lambda_1 + q_{32}\lambda_2), \\
L_8 =& -\frac{\pi^2 ah^2}{b}(C_{22} + e_{32}\lambda_1 + q_{32}\lambda_2) - \frac{\pi^2 bh^2}{4a}C_{66}, \\
L_9 =& -\frac{\pi^4 h^4}{128ab}\Bigg[2(C_{12} + 2C_{66}) \\
&+ \frac{9b^2}{a^2}(C_{11} + e_{31}\lambda_1 + q_{31}\lambda_2) \\
&+ \frac{9a^2}{b^2}(C_{22} + e_{32}\lambda_1 + q_{32}\lambda_2) + \lambda_1(e_{31} + e_{32}) \\
&+ \lambda_2(q_{31} + q_{32})\Bigg], \\
L_{10} =& -\frac{4h^3}{9abR_xR_y}\Bigg[3b^2R_y(C_{11} + e_{31}\lambda_1 + q_{31}\lambda_2) \\
&+ 3a^2R_x(C_{22} + e_{32}\lambda_1 + q_{32}\lambda_2) \\
&+ 3C_{12}(a^2R_y + b^2R_x) + a^2R_y(\lambda_1(e_{31} + 2e_{32}) \\
&+ \lambda_2(q_{31} + 2q_{32})) + b^2R_x(\lambda_1(2e_{31} + e_{32}) \\
&+ \lambda_2(2q_{31} + q_{32}))\Bigg], \\
L_{11} =& \frac{\pi^2 h^3}{3b}(C_{12} - C_{66} + e_{32}\lambda_1 + q_{32}\lambda_2) \\
&- \frac{2\pi^2 bh^3}{3a^2}(C_{11} + e_{31}\lambda_1 + q_{31}\lambda_2), \\
L_{12} =& \frac{\pi^2 h^3}{3a}(C_{12} - C_{66} + e_{31}\lambda_1 + q_{31}\lambda_2) \\
&- \frac{2\pi^2 ah^3}{3b^2}(C_{22} + e_{32}\lambda_1 + q_{32}\lambda_2), \\
L_{13} =& \frac{2ah^2}{3R_x}(C_{12} + e_{31}\lambda_1 + q_{31}\lambda_2)
\end{aligned} \tag{A.3}$$

$$+\frac{2ah^2}{3R_y}(C_{22}+e_{32}\lambda_1+q_{32}\lambda_2),$$

$$L_{14}=\frac{2bh^2}{3R_x}(C_{11}+e_{31}\lambda_1+q_{31}\lambda_2)+\frac{2bh^2}{3R_y}(C_{12}+e_{32}\lambda_1+q_{32}\lambda_2),$$

$$L_{15}=-\frac{1}{4}K\pi bhC_{55},\qquad L_{16}=-\frac{1}{4}K\pi ahC_{44},$$

$$L_{17}=-\frac{abh^2}{4R_x^2}(C_{11}+e_{31}\lambda_1+q_{31}\lambda_2)-\frac{abh^2}{4R_y^2}(C_{22}+e_{32}\lambda_1+q_{32}\lambda_2)-\frac{a\pi^2h^2}{4b}KC_{44}-\frac{b\pi^2h^2}{4a}KC_{55}-\frac{abh^2}{4R_xR_y}[2C_{12}+\lambda_1(e_{31}+e_{32})+\lambda_2(q_{31}+q_{32})],$$

$$L_{18}=-\frac{1}{4}I_0abh, \tag{A.4}$$

$$L_{19}=\frac{\pi^3h^4}{48b}[e_{24}e_{31}\delta_2-(e_{24}q_{31}+e_{31}q_{24})\delta_1+q_{24}q_{31}\delta_3]-\frac{\pi bh^2}{4}KC_{55}+\frac{\pi^3bh^4}{48a^2}[e_{15}e_{31}\delta_2-(e_{15}q_{31}+e_{31}q_{15})\delta_1+q_{15}q_{31}\delta_3],$$

$$L_{20}=\frac{\pi^2bh^3}{48a}[(e_{31}^2+e_{15}e_{31})\delta_2-C_{11}+(q_{31}^2+q_{15}q_{31})\delta_3-(e_{15}q_{31}+(q_{15}+2q_{31})e_{31})\delta_1]-\frac{\pi^2ah^3}{48b}C_{66}-\frac{abh}{4}KC_{55},$$

$$L_{21}=\frac{1}{48}\pi^2h^3[(e_{31}^2+e_{24}e_{31})\delta_2-C_{12}-C_{66}+(q_{31}^2+q_{24}q_{31})\delta_3-(e_{24}q_{31}+(q_{24}+2q_{31})e_{31})\delta_1], \tag{A.5}$$

$$L_{22}=\frac{\pi^3h^4}{48a}[e_{15}e_{32}\delta_2-(e_{15}q_{32}+e_{32}q_{15})\delta_1+q_{15}q_{32}\delta_3]-\frac{\pi ah^2}{4}KC_{44}+\frac{\pi^3ah^4}{48b^2}[e_{24}e_{32}\delta_2-(e_{24}q_{32}+e_{32}q_{24})\delta_1+q_{24}q_{32}\delta_3],$$

$$L_{23}=\frac{1}{48}\pi^2h^3[(e_{15}+e_{31})e_{32}\delta_2-C_{12}-C_{66}+(q_{15}+q_{31})q_{32}\delta_3-(q_{32}(e_{15}+e_{31})+(q_{15}+q_{31})e_{32})\delta_1],$$

$$L_{24}=\frac{\pi^2ah^3}{48b}[(e_{24}+e_{31})e_{32}\delta_2-C_{22}-(e_{32}(q_{24}+q_{31})+(e_{24}+e_{31})q_{32})\delta_1+(q_{24}+q_{31})q_{32}\delta_3]-\frac{\pi^2bh^3}{48a}C_{66}-\frac{abh}{4}KC_{44}. \tag{A.6}$$

For the closed-circuit boundary condition, we have the following equations.

$$L_1=\frac{\pi^2h^3}{6a^2b}[a^2(C_{12}-C_{66})-2b^2C_{11}],$$

$$L_2=\frac{2bh^2}{3R_x}C_{11}+\frac{2bh^2}{3R_y}C_{12},$$

$$L_3=-\frac{\pi^2bh^2}{a}C_{11}-\frac{\pi^2ah^2}{4b}C_{66},$$

$$L_4=-\frac{16h^2}{9}(C_{12}+C_{66}), \tag{A.7}$$

$$L_5=\frac{\pi^2h^3}{6a}(C_{12}-C_{66})-\frac{\pi^2ah^3}{3b^2}C_{22},$$

$$L_6=\frac{2ah^2}{3R_x}C_{12}+\frac{2ah^2}{3R_y}C_{22},$$

$$L_7=-\frac{16h^2}{9}(C_{12}+C_{66}),$$

$$L_8=-\frac{\pi^2ah^2}{b}C_{22}-\frac{\pi^2bh^2}{4a}C_{66}, \tag{A.8}$$

$$L_9=-\frac{\pi^4h^4}{128ab}\left[2(C_{12}+2C_{66})+\frac{9b^2}{a^2}C_{11}+\frac{9a^2}{b^2}C_{22}\right],$$

$$L_{10}=-\frac{4h^3}{9abR_xR_y}[3b^2R_yC_{11}+3a^2R_xC_{22}+3C_{12}(a^2R_y+b^2R_x)],$$

$$L_{11}=\frac{\pi^2h^3}{3b}(C_{12}-C_{66})-\frac{2\pi^2bh^3}{3a^2}C_{11},$$

$$L_{12}=\frac{\pi^2h^3}{3a}(C_{12}-C_{66})-\frac{2\pi^2ah^3}{3b^2}C_{22},$$

$$L_{13}=\frac{2ah^2}{3R_x}C_{12}+\frac{2ah^2}{3R_y}C_{22},$$

$$L_{14} = \frac{2bh^2}{3R_x}C_{11} + \frac{2bh^2}{3R_y}C_{12},$$

$$L_{15} = -\frac{1}{4}K\pi bhC_{55}, \qquad L_{16} = -\frac{1}{4}K\pi ahC_{44},$$

$$L_{17} = -\frac{abh^2}{4R_x^2}C_{11} - \frac{abh^2}{4R_y^2}C_{22} - \frac{a\pi^2h^2}{4b}KC_{44} - \frac{b\pi^2h^2}{4a}KC_{55} - \frac{abh^2}{2R_xR_y}C_{12},$$

$$L_{18} = -\frac{1}{4}I_0abh, \tag{A.9}$$

$$L_{19} = \frac{\pi^3h^4}{48b}[e_{24}e_{31}\delta_2 - (e_{24}q_{31} + e_{31}q_{24})\delta_1 + q_{24}q_{31}\delta_3] - \frac{\pi bh^2}{4}KC_{55} + \frac{\pi^3bh^4}{48a^2}[e_{15}e_{31}\delta_2 - (e_{15}q_{31} + e_{31}q_{15})\delta_1 + q_{15}q_{31}\delta_3],$$

$$L_{20} = \frac{\pi^2bh^3}{48a}[(e_{31}^2 + e_{15}e_{31})\delta_2 - C_{11} + (q_{31}^2+q_{15}q_{31})\delta_3-(e_{15}q_{31}+(q_{15}+2q_{31})e_{31})\delta_1] - \frac{\pi^2ah^3}{48b}C_{66} - \frac{abh}{4}KC_{55},$$

$$L_{21} = \frac{1}{48}\pi^2h^3[(e_{31}^2 + e_{24}e_{31})\delta_2 - C_{12} - C_{66} +(q_{31}^2+q_{24}q_{31})\delta_3-(e_{24}q_{31}+(q_{24}+2q_{31})e_{31})\delta_1], \tag{A.10}$$

$$L_{22} = \frac{\pi^3h^4}{48a}[e_{15}e_{32}\delta_2 - (e_{15}q_{32} + e_{32}q_{15}ht\delta_1 + q_{15}q_{32}\delta_3] - \frac{\pi ah^2}{4}KC_{44} + \frac{\pi^3ah^4}{48b^2}[e_{24}e_{32}\delta_2 - (e_{24}q_{32} + e_{32}q_{24})\delta_1 + q_{24}q_{32}\delta_3],$$

$$L_{23} = \frac{1}{48}\pi^2h^3[(e_{15} + e_{31})e_{32}\delta_2 - C_{12} - C_{66} + (q_{15} + q_{31})q_{32}\delta_3 - (q_{32}(e_{15} + e_{31}) + (q_{15} + q_{31})e_{32})\delta_1],$$

$$L_{24} = \frac{\pi^2ah^3}{48b}[(e_{24} + e_{31})e_{32}\delta_2 - C_{22} - (e_{32}(q_{24} + q_{31}) + (e_{24} + e_{31})q_{32})\delta_1 +(q_{24}+q_{31})q_{32}\delta_3] - \frac{\pi^2bh^3}{48a}C_{66} - \frac{abh}{4}KC_{44}. \tag{A.11}$$

Appendix B

$$g_1 = (L_{21}L_{22} - L_{19}L_{24})/(L_{20}L_{24} - L_{21}L_{23}),$$

$$g_2 = (L_{19}L_{23} - L_{20}L_{22})/(L_{20}L_{24} - L_{21}L_{23}),$$

$$g_3 = (L_4L_6 - L_2L_8)/(L_3L_8 - L_4L_7),$$

$$g_4 = (L_4L_5 - L_1L_8)/(L_3L_8 - L_4L_7),$$

$$g_5 = (L_2L_7 - L_3L_6)/(L_3L_8 - L_4L_7),$$

$$g_6 = (L_1L_7 - L_3L_5)/(L_3L_8 - L_4L_7),$$

$$\omega_0 = \sqrt{(L_{17}+L_{13}g_5+L_{14}g_3+L_{15}g_1+L_{16}g_2)/L_{18}},$$

$$\alpha = (L_{10} + L_{11}g_3 + L_{12}g_5 + L_{13}g_6 + L_{14}g_4)/L_{18},$$

$$\beta = (L_9 + L_{11}g_4 + L_{12}g_6)/L_{18}.$$

Biographies

Alireza Shooshtari is Associate Professor of Mechanical Engineering at Bu-Ali Sina University. He received his BS degree in Mechanical Engineering from Tehran University, Tehran, Iran; and his MS and PhD (2006) degrees in Applied Mechanics, respectively, from Bu-Ali Sina University, Hamedan, Iran, and Tarbiat Modarres University, Tehran, Iran. His research interests are nonlinear dynamics of engineering structures, modal analysis, and random vibrations.

Soheil Razavi is candidate for the PhD degree in Applied Mechanics. He received his MSc in Applied Mechanics from Bu-Ali Sina University, Hamedan, Iran, in 2010. His MSc thesis was about single-mode analysis of hybrid laminated plates. His PhD dissertation deals with the analytical study of nonlinear dynamics of smart plates and shells.